# Dependence of axon diameter index on maximum gradient strength

**T. B. Dyrby[1], P. L. Huppard[2], M. Ptito[3], M. G. Hall[4], and D. C. Alexander[4]**
[1]Danish Research Centre for Magnetic Resonance, Copenhagen Univerviersity Hospital, Hvidovre, Denmark, [2]Imaging Science and Biomedical Imaging, University of Manchester, Manchester, United Kingdom, [3]School of Optometry, University of Montreal, Montreal, Canada, [4]Centre for Medical Image Computing, University College London, London, United Kingdom

**Introduction:** The active imaging algorithm [1] optimises diffusion MRI protocols for mapping axon diameter without knowledge of fibre orientation and from a sparse set of measurements. The idea potentially provides new and valuable indices of axon diameter from images acquired from live subjects using standard clinical scanners [5]. However, the method in [5] provides only a single summary statistic, or index, of the distribution of axon diameters in white matter and the nature of the index remains unclear. Here we study the dependence of the axon diameter index on the maximum gradient strength $G_{max}$ available on the scanner. We used an experimental MR scanner with $G_{max}$ up to 400mT/m, but optimised protocols for various smaller $G_{max}$, acquired data on a fixed tissue sample and compared maps of the axon diameter index.

**Method:** We used the experiment design framework in [1] to tune multi-shell HARDI protocols for simultaneous sensitivity to a priori axon diameters of 1, 2 and 4 μm. The procedure provides three unique combinations of gradient strength (G), pulse-width (δ) and the pulse separation (Δ). A simple extension to the framework determines the optimal division of 360 measurements into different sized sets of gradient directions for each combination and b=0 measurements. Four optimal protocols for fixed monkey brain tissue on a 4.7T Varian experimental MR scanner were designed with different maximum gradient strength $G_{max}$ of 60, 140, 200 and 300 mT/m. The three unique *b* values at each $G_{max}$ are [1355, 2368, 5415], [2007, 3368, 9422], [2242, 3791, 11329] and [2421, 4609, 111329] s/mm$^2$, respectively and acquired in [91, 99, 102], [98, 105, 87], [100, 105, 84] and [102, 105, 82] gradient directions. The remaining images in each optimised protocol have b=0 to make the total 360, NEX=1, 30 sagittal slices covering the mid-sagittal plane of corpus callosum (CC), TR=2500 ms, isotropic 0.5 mm voxels, and TE was [71.5, 52, 46, 39.1] ms. Data were acquired on a fixed Vervet monkey brain prepared as [6] in a scanning session lasting 168 hrs. While scanning, the temperature around the tissue was 20°C (±1°C). We fit a four-compartment model, derived from the three-compartment white-matter models of [2,4], as in [5], to each of the acquired datasets to obtain a single index of axon diameter in each voxel. For data analysis, the midsagittal plane of the CC was subdivided into 10 regions as in [7]. Accompanying simulation experiments were used to give insight into the sensitivity of each optimised protocol to a wide range of true axon diameters.

**Results:** Figure 1 shows that, for each $G_{max}$, the axon diameter index within regions of the CC follows the low-high-low trend known from histological data [7,8]. However, in comparison to the mean axon diameter weighted by axon volume, which we might expect the index to approximate, the axon diameter index is consistently about twice as high as for histological data. Overestimation is most significant for the lowest $G_{max}$ of 60 mT/m. The results stabilise at higher $G_{max}$ (>60 mT/m), although the standard error decreases steadily as $G_{max}$ increases. Figure 2 shows maps of the axon diameter index at $G_{max}$ of 140, 200 and 300 mT/m, which illustrates the difference in noise level nicely. The $G_{max}$ = 300 mT/m map is less noisy and has higher spatial coherence and contrast in the 1.5-5 μm range. Simulations in figure 3 support the findings in figures 1 and 2. Axons diameters less than about 3 μm appear indistinguishable for low $G_{max}$ (60 mT/m) but smaller diameters become more distinguishable as $G_{max}$ increases.

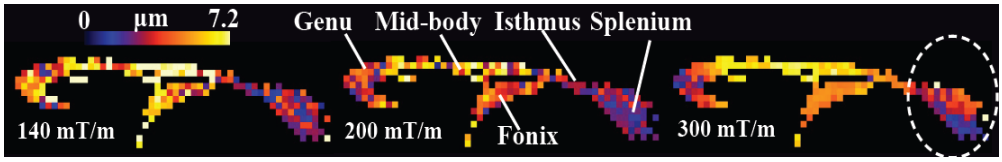


**Fig. 2: Axon diameter index map in the midsagittal plan of the CC with a $G_{max}$ of 140 (left), 200 and 300mT/m. Results improves with higher $G_{max}$ as seen in e.g. the region of splenium (circle).**

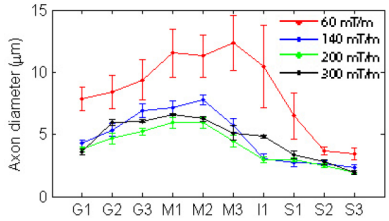


**Fig. 1: Maps of mean axon diameter (±standard error) versus $G_{max}$ shown in sub-region of CC from anterior: G1-3 (genu), M1-3 (mid-body), I (isthmus) and S1-3 (splenium).**

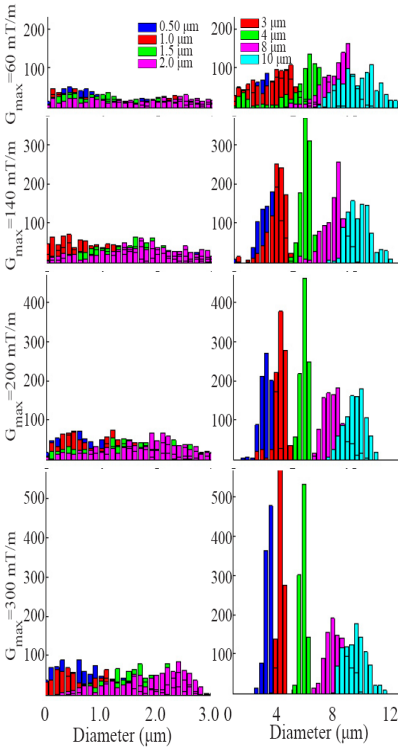


**Fig. 3: Posterior distributions on various true axon diameters from each optimised protocol using the MCMC procedure in [1].**

**Acknowledgment:**
The Lundbeck Foundation

**Discussion and conclusion:** The axon diameter index is sensitive to available $G_{max}$, but we observe good consistency for $G_{max}$ = 140mT/m and above. For the lowest $G_{max}$ of 60 mT/m, the axon diameter index is skewed towards higher values, because of lack of sensitivity to lower diameters. However, as $G_{max}$ increases to 140 mT/m and above we gain sensitivity to the full a priori range of axon diameters used in the experiment design optimization. As $G_{max}$ increases above 140 mT/m, the gain is largely just in SNR which reduces noise without changing the axon diameter indices significantly. However, we expect that larger $G_{max}$ enables tuning of the protocol for smaller a priori axon diameter values, which increases the sensitivity of the axon diameter index to smaller populations of axons. Further work will consider which populations of a priori axons diameters are important to target for specific applications and determine which $G_{max}$ is required for optimal sensitivity to each population.

**References** *1 Alexander MRM08, 2 Stanisz MRM95. 3 Assaf MRM08. 4 Barazany BRAIN09. 5 Alexander ISMRM09, 6 Dyrby ISMRM08. 7 Aboitiz B. Res. 92. 8 Lamantia JCN90.*